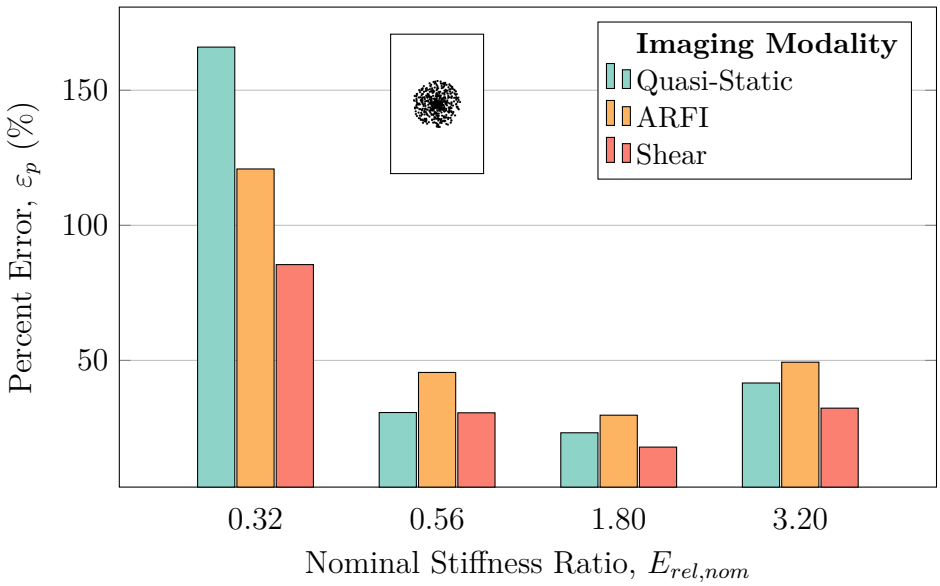

Fig. 6.6: Percent error of measured stiffness ratios for clustered lesions with a cluster density of $20\,\mathrm{cm}^{-2}$ and individual radii of 1 mm across the three investigated modalities.

superior to the ischial tuberosity—a boney prominence often associated with deep tissue injuries. As Fig. 6.7 shows, shear wave speed quantification once again presented the most ideal detection sensitivity of the three modalities. Both quasi-static elastography and ARFI imaging were much less sensitive to lesions in this model, with unstiff lesions being almost impossible to detect using quasi-static elastography. A key differentiation in this Visible Human model from the hard-boundaried spherical model studied previously is that shear wave speed quantification grossly underestimated the stiffness of both the least stiff and stiffest lesions examined.

As Fig. 6.8 shows, the error for shear wave speed quantification is much greater for both very unstiff ($E_{rel,nom} = 0.32$) and very stiff ($E_{rel,nom} = 3.20$) lesions—the error for unstiff lesions even surpasses that of ARFI imaging for the first time. For all other nominal stiffness ratios, shear wave speed quan-

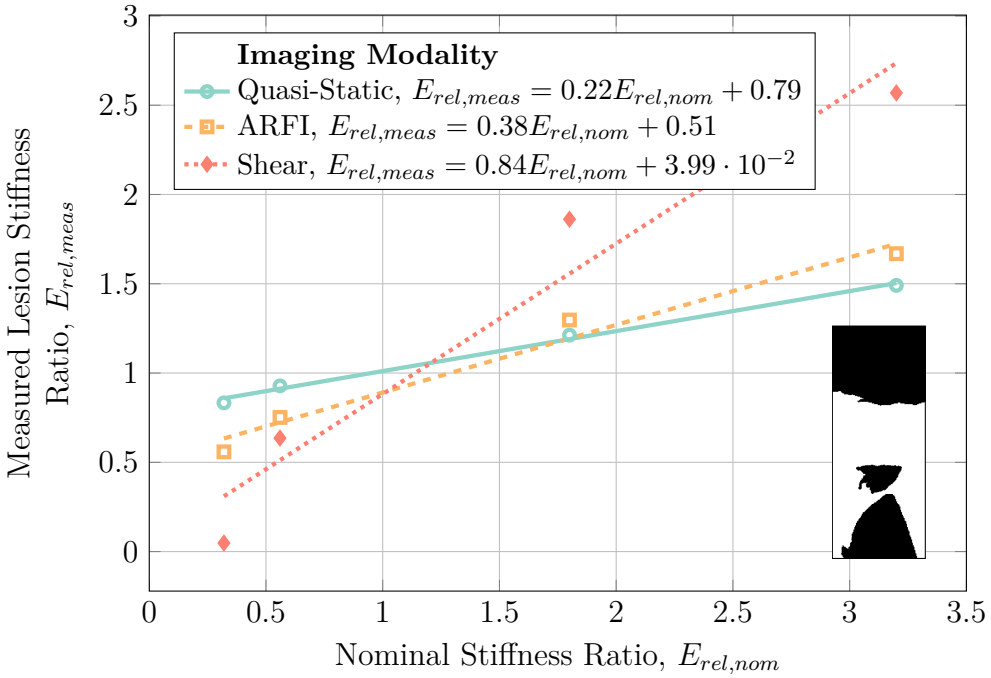

Fig. 6.7: Detection sensitivities of MRI-acquired Visible Human lesions with a width of 20 mm at a depth of 6 cm using quasi-static elastography, ARFI imaging, and shear wave speed quantification.

tification once again outperformed both quasi-static elastography and ARFI imaging. Although the use of more complicated geometry in the Visible Human project decreased the accuracy of shear wave speed quantification, it was once again the most sensitive and accurate of the investigated imaging modalities, suggesting it be used for quantifying deep tissue injuries if at all possible.

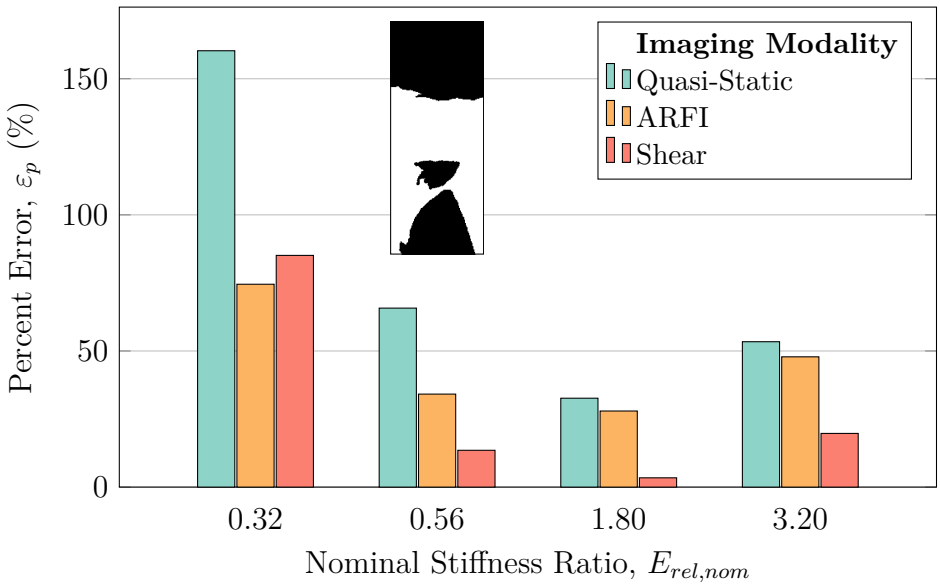

Fig. 6.8: Percent error of measured stiffness ratios for MRI-acquired Visible Human lesions with a width of 20 mm at a depth of 6 cm across the three investigated modalities.

Experimental Validations

In the experiments that were performed with each of the three elastography modalities on a tissue mimicking phantom, all three methodologies were able to distinguish both hard and unstiff lesions with some degree of accuracy. However, the stiffest lesions that were examined—those with a nominal stiffness ratio of 3.2—presented the greatest error and variation in the results as seen in Fig. 6.9. In these experiments, both ARFI imaging and shear wave speed quantification score similarly, although the variation in the shear results was much greater than the variation in the ARFI experiments. Both ARFI imaging and shear wave speed quantification showed relatively similar detection sensitivities with the major difference between the two being that ARFI imaging consistently over-estimated lesion stiffness as compared to shear wave speed quantification. Shear wave speed quantification was found to be the most accu-

rate for unstiff lesions, while ARFI imaging performed marginally better with stiff lesions. Quasi-static elastography generally displayed the worst results, echoing what was seen in Section 6.1.

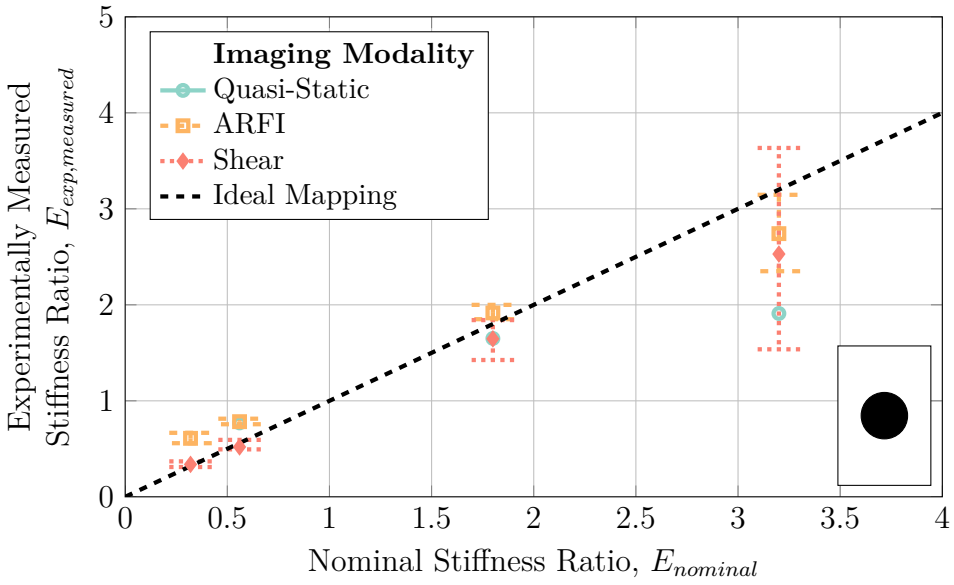

Fig. 6.9: Experimental results of the three methodologies investigated. ARFI imaging consistently overestimated the stiffness of the lesion compared to both quasi-static and shear wave speed quantification, which generally underestimated the stiffness of lesions.

By comparing the simulated results presented throughout this work to the parametrically identical results obtained through experiment, the accuracy of the simulations apart from the overall accuracy of the technique may be determined. These results are compared in Fig. 6.10 which shows a general agreement between experimentally measured stiffness ratios and their simulated counterparts for all but stiff ARFI imaging-acquired lesions. Since the simulation results for quasi-static elastography and shear wave speed quantification fall within error of their experimental counterparts, these simulation paradigms may be deemed acceptable. Counter to this, the simulation-acquired stiffness ratios in ARFI imaging fall well below their experimental values, suggesting

that the current ARFI imaging simulation methodology is insufficient in accurately reproducing real-world results and that future work is necessary to more closely align the ARFI imaging models with reality.

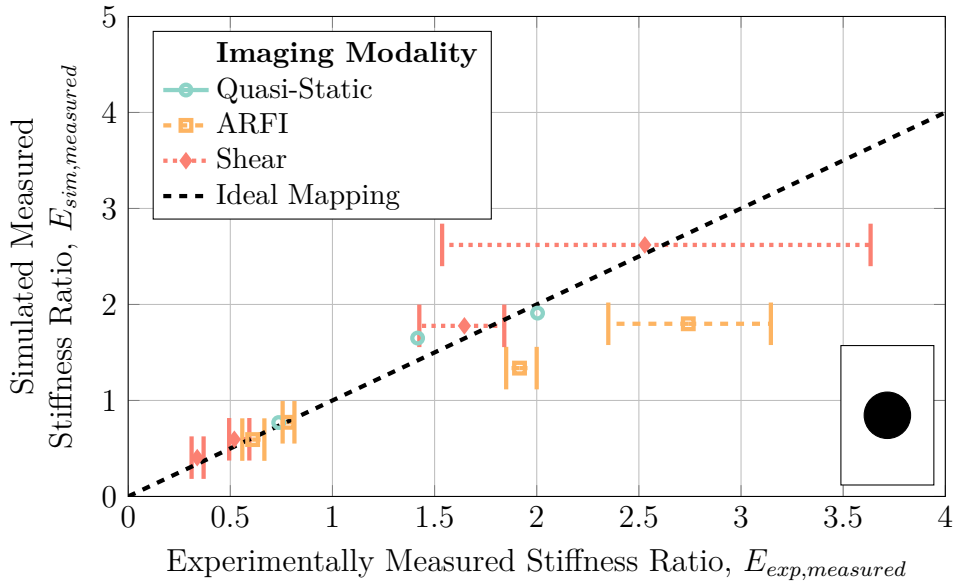

Fig. 6.10: Experimental validation of the simulation results across all three methodologies investigated. The quasi-static ultrasound elastography and shear wave speed quantification simulations most closely matched the results seen experimentally.

6.2 Recommendations and Future Work

The work presented in Chapters 3 – 5 represents a numerical characterization of three different ultrasound elastography imaging modalities: quasi-static ultrasound elastography, acoustic radiation force impulse imaging, and shear wave speed quantification. From the results presented in these chapters the critical parameters relating to detecting both formative and progressive deep tissue injuries across all three detection modalities were investigated. These parameters included device-design specifics such as: frequency; transmit pres-